SINGLE LINK ROBOT ACTUATED WITH SHAPE MEMORY ALLOY

Nicu-George Bîzdoacă,
Daniela Pană, Sonia Degeratu, Elvira Bîzdoacă,
Cristina Pană, Marius Niculescu

University of Craiova, Faculty of Control, Computers and Electronics,
5 Tehnicii, 1100 Craiova
E-mail: nicu@robotics.ucv.ro

Abstract: The present paper explore the robotics control actuation using shape memory alloy tendon. Shape memory alloy offer an interesting solution, using the shape transformation of the wire/structure in the moment of applying a thermal type transformation able to offer the martensitic temperature. This thermal transformation can be inducted using electrical current and a suitable control strategy.
In order to assure an efficient control of SMA actuator applied to inverted pendulum, a mathematical model and numerical simulation of the resulting model is required. Due a particular possibility SMA actuator connection, a modified dynamics for wire or tendon actuation is presented. The control possibilities are explored: PI, PD and PID controller are connected to the single link SMA actuation. Numerical simulations are presented and observations are formulated.

Key words: Robotics, numerical simulation, shape memory alloy actuation, mathematical model.

1. SHAPE MEMORY ALLOY

The shape memory effect was first noted over 50 years ago; it was not until 1962, however, with the discovery of a nickel titanium shape memory alloy but Buehler, that serious investigations were undertaken to understand the mechanism of the shape memory effect. The shape memory alloys possess the ability to undergo shape change at low temperature and retain this deformation until they are heated, at which point they return to their original shape. The nickel titanium alloys, used in the present research, generally refereed to as Nitinol, have compositions of approximately 50 atomic % Ni/ 50 atomic % Ti, with small additions of copper, iron, cobalt or chromium. The alloys are four times the cost of Cu-Zn-Al alloys, but it possesses several advantages as greater ductility, more recoverable motion, excellent corrosion resistance, stable transformation temperatures, high biocompatibility and the ability to be electrically heated for shape recovery.
Shape memory actuators are considered to be low power actuators and such as compete with solenoids, bimetals and to some degree was motors. It is estimated that shape memory springs can provide over 100 times the work output of thermal bimetals.
The use of shape memory alloy can sometimes simplify a mechanism or device, reducing the overall number of parts, increasing reliability and therefore reducing associated quality costs. Because of its high rezistivity of 80 – 89 micro ohm-cm, nickel titanium can be self heated by passing an electrical current through it. The basic rule for electrical actuation is that the temperature of complete transformation to martensite Mf, of the actuator, must be well above the maximum ambient temperature expected.
The alloys and manufacturing techniques improved, the experience and results of experimenters open the gates to the commercial applications. Nitinol received much attention for medical applications, toys industry, teleoperated systems and robotics, especially autonomous robots. In 1989 Oaktree Automation Inc, in Alexandria Virginia, started developing the Finger spelling Hand, an anthropomorphic robotic device to serve as a tactile communication aid for deaf - blind individuals, particularly those unable to read Braille. The device used a total of one hundred and eight 250 μm Flexinol wires acting in parallel.
Based on description of shape memory alloy materials, a SMA Simulink block was developed. The characteristic of material is idealized, but the approximations made are suitable for an efficient simulation. The user can indicate the start and stop martensitic and austenitic temperature and the force, momentum evolution.

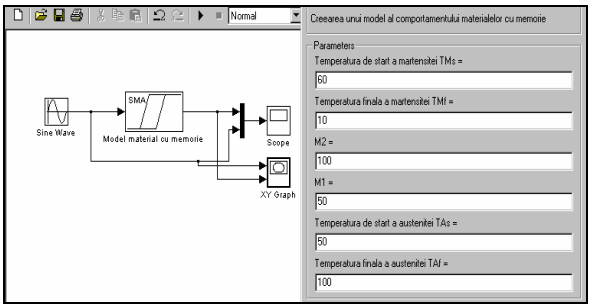

Fig. 1. Configurable model for shape memory alloy wire actuator

The numerical results respect the real comportment of the user specified shape memory alloy:

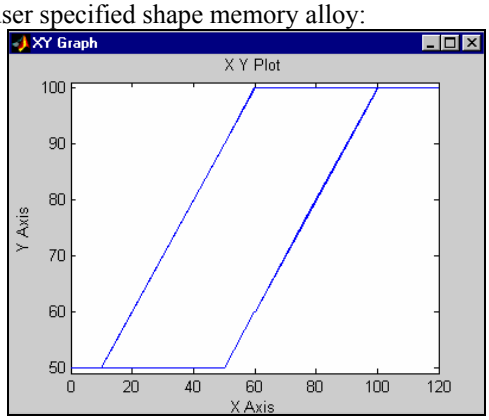

Fig. 2.The simulation result for SMA material response

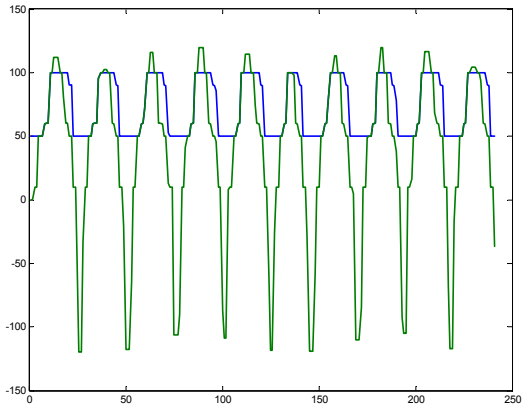

Fig. 3. The simulation result for shape memory alloy wire actuator

The electrical activation of SMA actuator imposes the following relations for the current, temperature and response time:
For heating

$$T_{Max} = 4{,}928\frac{I}{d} + 1{,}632\frac{I^2}{d^2} = K_{T1}\frac{I}{\sqrt{F_L}} + K_{T2}\frac{I^2}{F_L} \quad (1.)$$

T_{Max} - maximum temperature, d – wire diameter, I – electrical current, FL - required force

$$t_{Heating} = J_h \ln\frac{T_{Max} - T_{medium}}{T_{Max} - T} \quad (2.)$$

$t_{Heating}$ – heating time, J_h – heating coefficient, T_{medium} – medium temperature, TA – ambient temperature, T - aim temperature upon heating

$$J_h = 6{,}72 + 3{,}922d^2 = K_{J_1} + K_{J_2}F_L \quad (3.)$$

For cooling

$$t_c = J_c \ln\frac{T_H - T_A}{T_c - T_A} + \frac{28{,}88}{M_S - T_A} \quad (4.)$$

$$J_c = 4{,}88 + 6{,}116d^2 = K_{J_{c1}} + K_{J_{c2}}F_L \quad (5.)$$

t_c – cooling time, T_H - initial temperature upon cooling, T_A - ambient temperature, d –wire diameter, T_C - aim cooling temperature, J_C - time constant for cooling, M - martensitic start temperature.
One can observe the time dependence of required force and required stroke.
The electrical calculations for direct current heating determine:

- The amount of current needed for actuation in the required time
- The resistance of the nickel titanium actuation element
- The voltage required to drive the current through element
- The power dissipated by the actuation element.

The first requirement can be establish using the material description tables (Waram 1993).
The resistance is determined using the following expression:

$$Resistance/mm = \frac{1{,}019x10^{-3}}{d^3}\Omega/mm \quad (6.)$$

The voltage and power requirements results from:

$$V = IR\ ;\ Power = I^2R \quad (7.)$$

I – current in amps, V voltage in volts, R resistance in Ω.
In case of using pulse width modulation heating the following relation can be used:

$$duty\ cycle(\%) = \frac{t_1}{t_2}x100 \quad (8.)$$

t_1 – the width of constant current pulse, t_2 the total cycle time.

$$duty\ cycle(\%) = \frac{100}{I_i}\sqrt{\frac{P_{avr}}{R}} \quad (9.)$$

$$duty\ cycle(\%) = \frac{100}{V_i}\sqrt{P_{avr}R} \quad (10.)$$

P_{avg} – average pulsed power (effective DC power), I_i applied pulse current, V_i applied pulsed voltage, R electric resistance.

2. DYNAMICS OF ONE AXIS ROBOT (INVERTED PENDULUM)

Consider the one-axis robot or inverted pendulum shown in Figure 4. One assumes that the link is a thin cylinder or rod of mass m_1.
There are many methods for generating the dynamic equations of mechanical system. All methods generate equivalent sets of equations, but different forms of the equations may be better suited for computation different forms of the equations may be better suited for computation or analysis. The Lagrange analysis will be used for the present analysis, a method which relies on the energy proprieties of mechanical system to compute the equations of motion.
Letting $v_i \in R^3$ be the translational velocity of the center of mass for the ith link and $\omega_i \in R^3$ be angular velocity, the kinetic energy of the manipulator is:

$$T(\theta,\dot{\theta}) = \frac{1}{2} m_1 \|v_1\|^2 + \frac{1}{2} m_1 \omega_1^T I_1 \omega_1 \qquad (11.)$$

Since the motion of the manipulator is restricted to xy plane, $\|v_i\|$ is the magnitude of xy velocity of the centre of mass and ω_i is a vector in the direction of the y axis, with $\|\omega_1\| = \dot{\theta}_1$.

We solve for kinetic energy in terms of the generalized coordinates by using the kinematics of the mechanism. Let denote the position of the ith centre of mass.

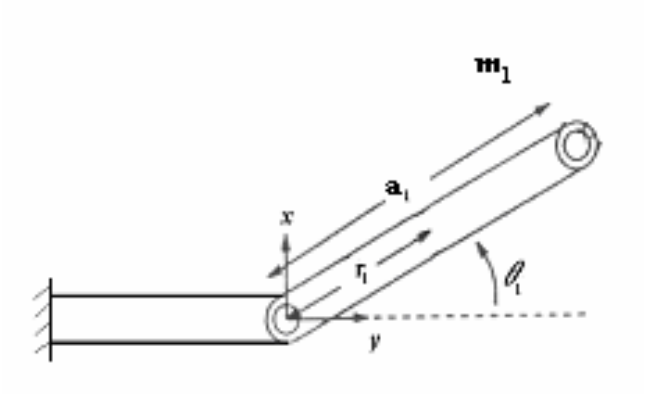

Fig. 4 . Two link finger architecture

If r_1 is the distance from the joints to the centre of mass for link, results

$$x_1 = r_1 \cos(\theta_1) \qquad (12.)$$

$$y_1 = r_1 \sin(\theta_1) \qquad (13.)$$

$$\dot{x}_1 = -r_1 \dot{\theta}_1 \sin(\theta_1) \qquad (14.)$$

$$\dot{y}_1 = r_1 \dot{\theta}_1 \cos(\theta_1) \qquad (15.)$$

Using the kinetic energy and Lagranage methods results:

$$\tau_1 = \left(\frac{m_1 a_1^2}{3}\right)\ddot{\theta}_1 + \frac{g m_1 a_1 \cos(\theta_1)}{2} + b_1(\theta_1) \qquad (16.)$$

with

$$b_1(\theta_1) = b_1^v \dot{\theta}_1 + \operatorname{sgn}(\dot{\theta}_1)\left[b_1^d + (b_1^s - b_1^d)\exp\frac{-|\dot{\theta}_1|}{\varepsilon}\right]$$

b_1^v - viscous friction coefficient

b_1^d - dynamic friction coefficient

b_1^s - static friction coefficient

ε - small positive parameter

3. SHAPE MEMORY ACTUATOR STRUCTURE

Due the actuation architecture a simple mathematical model can be establish. Schematically the shape memory actuation is:

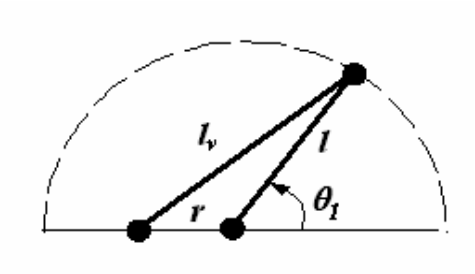

Fig. 5 . Shape memory alloy actuation structure

In Figure 5 the l_v is the variable length of shape memory alloy wire, the l is the robotic link length between the articulation point and the shape memory alloy wire connection, r is the distance between the second end of the SMA wire (which is a fixed point) and the articulation point of the link (fixed point too).

Using simple mathematical computation the mathematical dependence can be established:

$$\theta_1 = \arccos\left(\frac{l_v^2 - (r^2 + l^2)}{2lr}\right)$$

$$\Leftrightarrow \theta_1 = f(l_v^2)$$

The graphic of θ_1 as function of l_v is the following, considering the real domain variation for $\theta_1 \in [0, \pi]$.

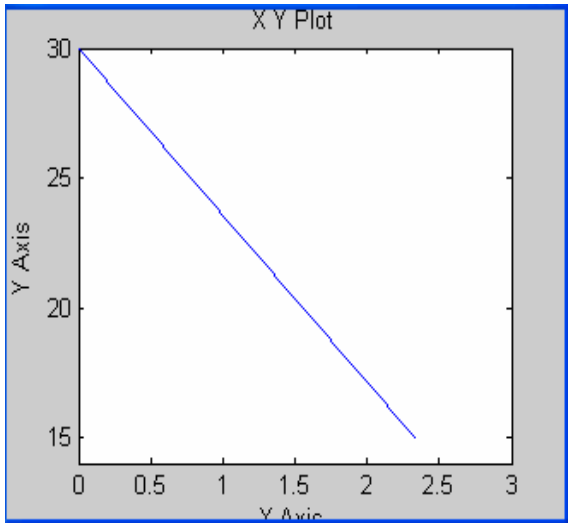

Fig. 6. The graphic $l_v = f(\theta_1)$.

As can easily see the dependence is linear, that the liniarisation in modeling can be done successfully.

The explanations concern the structural variation of SMA actuator, which are limited superior by l_v and inferior by 0.5 l_v.

The mathematical model including the SMA actuation can be developed in two ways:

First is possible to consider for position control**, ONLY** the length variation of the SMA actuator. This approach is a correct one, the additional torque, provided by the particular proprieties of SMA, enforces the actuation. The situation corresponds to tendon actuation or wire actuation.

Using the substitution:

$$\dot{\theta}_1 = \frac{-2l_v}{lr\sqrt{4-\left(\frac{l_v^2-l^2-r^2}{lr}\right)^2}}\dot{l}_v \qquad (17.)$$

$$\ddot{\theta}_1 = \frac{-2l_v}{lr\sqrt{4-\left(\frac{l_v^2-l^2-r^2}{lr}\right)^2}}\ddot{l}_v - \frac{2}{lr\sqrt{4-\left(\frac{l_v^2-l^2-r^2}{lr}\right)^2}}\dot{l}_v^2 - \frac{4l_v^2\left(l_v^2-l^2-r^2\right)}{l^3r^3\sqrt{\left(4-\left(\frac{l_v^2-l^2-r^2}{lr}\right)^2\right)^2}}\dot{l}_v^2 \qquad (18.)$$

the mathematical model of the single link robot with wire actuation is:

$$\tau_1 = \left(\frac{m_1a_1^2}{3}\right)\left(\frac{-2l_v}{lr\sqrt{4-\left(\frac{l_v^2-l^2-r^2}{lr}\right)^2}}\ddot{l}_v - \frac{2}{lr\sqrt{4-\left(\frac{l_v^2-l^2-r^2}{lr}\right)^2}}\dot{l}_v^2 - \frac{4l_v^2\left(l_v^2-l^2-r^2\right)}{l^3r^3\sqrt{\left(4-\left(\frac{l_v^2-l^2-r^2}{lr}\right)^2\right)^2}}\right) + \frac{gm_1a_1\left(l_v^2-\left(r^2+l^2\right)\right)}{4lr} + b_1(\theta_1) \qquad (19.)$$

Analyzing the equilibrium conditions, results that $\tau_1 = b_1(\theta_1)$ and $l_v^2 = r^2 + l^2$, state which correspond to real case.

Second way makes a simplifying assumption: because the SMA connection with single link structure can be choose near to the articulation point, we can assume that the entire SMA torque is directly used for movement. Then the mathematical model can be expressed as:

$$\tau_{SMA} = \left(\frac{m_1a_1^2}{3}\right)\ddot{\theta}_1 + \frac{gm_1a_1\cos(\theta_1)}{2} + b_1(\theta_1) \qquad (20.)$$

4. NUMERICAL SIMULATIONS

Based on the theoretical background presented, numerical simulations are required in order to evaluate the efficiency of real mechanism. For flexible studies all the elements are developed as configurable Simulink blocks:

- Shape memory alloy wire – block presented in the first part of article
- Dynamics of inverted pendulum block – based on 11. - 20. equations:

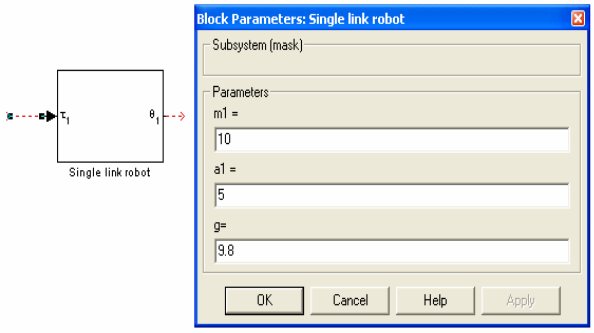

Fig. 7. Dynamics of single link robot in configurable block.

Connecting all this blocks , for numerical simulations the following parameters are used:

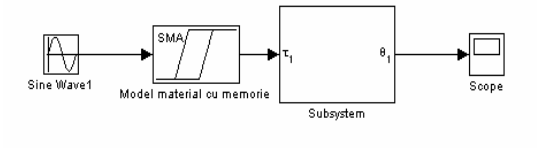

Fig. 8. Simulation blocks for shape memory alloy actuated pendulum.

mass =m_1= 1 kg
length = a_1= 0.5 m
gravity = 9.8 m/s2

- shape memory alloy parameters:
  start temperature of martensitic state = 60^0C
  final temperature of martensitic state = 10^0C
  start temperature of austenite state = 50^0C
  final temperature of austenite state = 100^0C
  lower force M1 = .05 N
  higher force developed by the SMA M_2 = 5 N

The results of numerical simulations are:

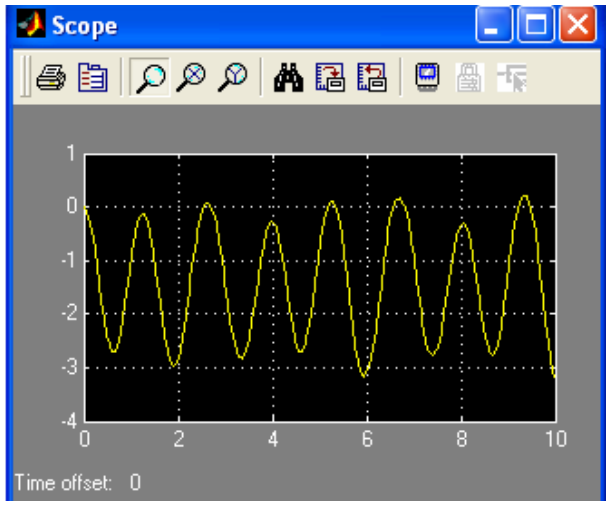

Fig 9. Numerical results for sinusoidal excitation of the SMA actuated pendulum

The evolution of q1 angle is near sinusoidal evolution. These conclude that the control procedure can be a conventional one, as a PI, PD or a PID controller. In order to explore these possibilities we have made numerical simulation for simple controller.

- First we try a P controller with K_P=30.

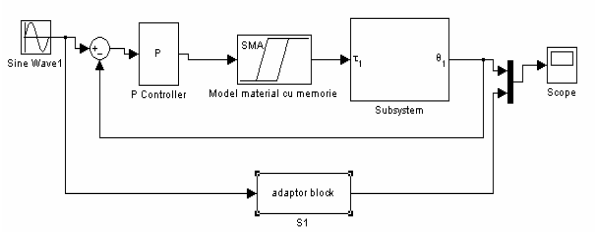

Fig. 10. P controller for shape memory alloy actuated pendulum.

The evolution conduct to a significant error, which conclude that a more complex controller is required.

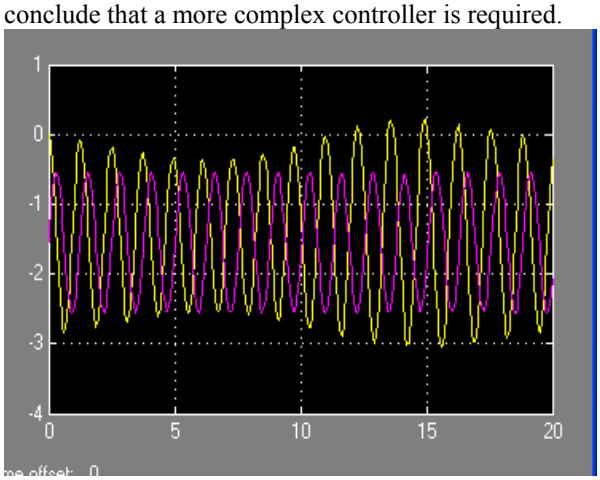

Fig. 11. $\theta_{references}$ (red) and θ_1 (yellow) evolution for P controller.

The second controller used in numerical simulation was a PI controller, with K_P = 10, K_I=5.

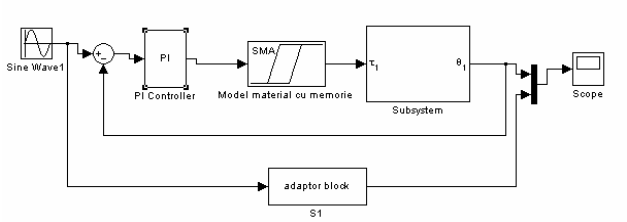

Fig. 12 . PI controller for shape memory alloy actuated pendulum.

The integrator component was not a suitable solution, the system response being unacceptable.

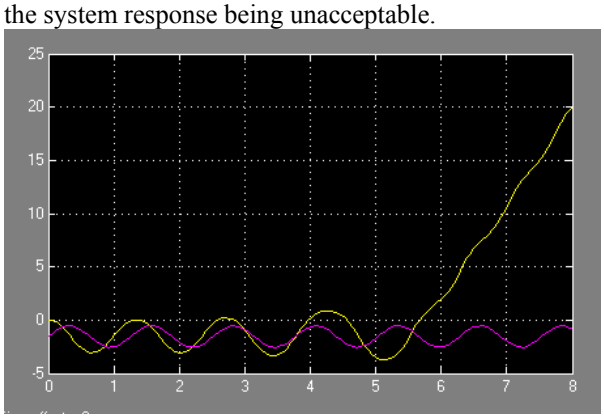

Fig. 13 . $\theta_{references}$ (red) and θ_1 (yellow) evolution for PI controller.

- Using now a PID controller, with a strong derivative component and a small integrator constant: K_P=10, K_D=70, K_I=.005, the complete structure will have the components:

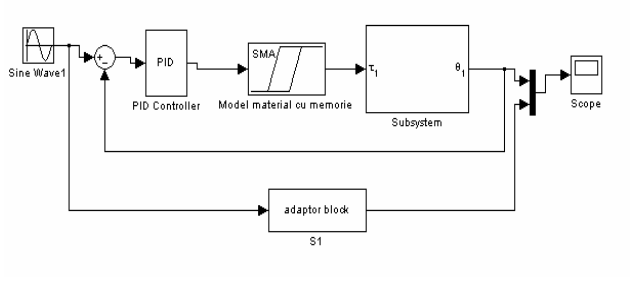

Fig. 14 . PID controller for shape memory alloy actuated pendulum.

The system response is improved and the performance are suitable for a real and suitably applications:

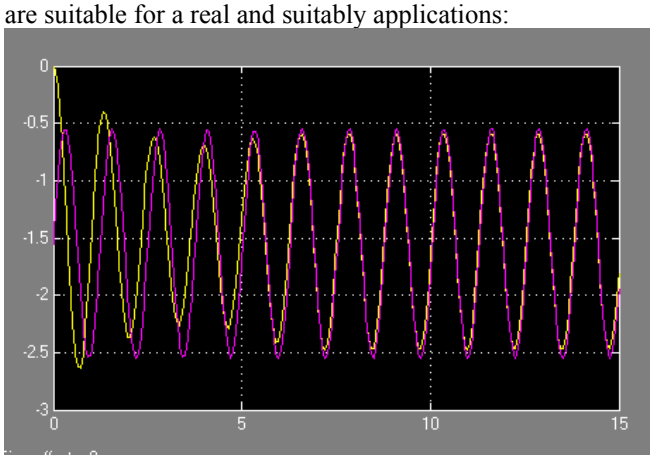

Fig. 15 . $\theta_{references}$ (red) and θ_1 (yellow) evolution for PID controller.

5. CONCLUSIONS

The simulations and the mathematical model developed in the article offer a background in studying the single link robotic control possibilities. The results respect the real evolution of the structure. In the future, the authors will explore all the control possibilities applied to a real model; witch for the moment is under construction.

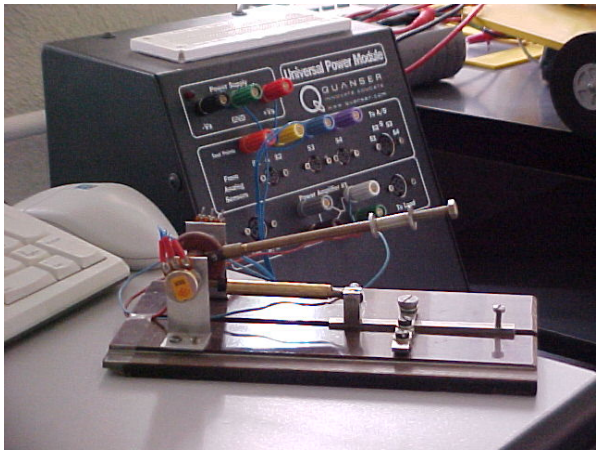

Fig. 16. Experimental model for a single link robotic structure

REFERENCES

Bîzdoacă N, Diaconu I. (2001), Hierarchical Control of a Smart Material Hyperredundant Cooperative Robots, *ISR 2001*, Seoul, South Korea.

Bîzdoacă N, Diaconu I. (2003) Shape memory alloy hyper-redundant robotic structure, *CMM 2003*, Gliwice, Poland.

Delay L, Chandrasekaran M. (1987), *Les Editions Physique*, Les Ulis

Graesser E.J., Cozarelli F.A.(994), *Journal of Intelligent Material Systems and Structures.*

Ivănescu M, Bîzdoacă N.(2000), An Intelligent Control System for Hyperredundant Cooperative Robots, *ISRA 2000*, Monterrey, Mexico.

Ivănescu M.(1986), A New Manipulator Arms - A Tentacle Model, *Recent Trends in Robotics*.

Schroeder B., Boller Ch.(1998), Comparative Assessment of Models for Describing the Constitutive Behaviour of Shape Memory Alloy, *Smart Materials and Structures*.

Stalmans R.(1993), *Doctorate Thesis*, Catholic Univ. of Leuven, Dep. Of Metallurgy and Materials Science, 1993

Waram T. (1993), *Actuator Design Using Shape Memory Alloys*

Murray R.,Li Z., Sastry S.(1993), *A mathematical introduction to robotic manipulation*, CRC Press.